Direct Imaging of Asymmetric Magnetization Reversal in Exchange-Biased Fe/MnPd Bilayers by X-Ray Photoemission Electron Microscopy

P. Blomqvist and Kannan M. Krishnan*
Materials Science and Engineering, University of Washington, Seattle, Washington 98195, USA

H. Ohldag
Stanford Synchrotron Radiation Laboratory, Stanford University, Stanford, California 94025, USA
(Received 27 October 2004; published 16 March 2005)

X-ray photoemission electron microscopy is used to probe the remnant magnetic domain structure in high quality, single-crystalline, exchange-biased Fe/MnPd bilayers. It is found that the induced unidirectional anisotropy strongly affects the overall magnetic domain structure. Real space images of the ferromagnetic domains provide direct evidence for an asymmetric magnetization reversal process after saturation along the ferromagnetic hard direction. The magnetization reversal occurs by moment rotation for decreasing fields while it proceeds by domain nucleation and growth for increasing fields. The observed domains are consistent with the crystallography of the bilayers and favor a configuration that minimizes the overall magnetostatic energy of the ferromagnetic layer.

DOI: 10.1103/PhysRevLett.94.107203 PACS numbers: 75.60.Jk, 68.37.Yz, 75.70.–i, 81.15.Hi

The exchange bias effect is a result of the coupling at the interface between a ferromagnet (FM) and an antiferromagnet (AFM) that have been field cooled through the Néel temperature. This exchange bias (EB), represented by a shifted magnetic hysteresis loop, and found in many AFM/FM bilayer systems [1–3], shows a variety of unusual behaviors that include enhanced coercivity [4], magnetic training effects [5], perpendicular coupling [6], kinked hysteresis loops [7,8] and an asymmetry in the magnetization reversal process [8–12]. A number of theoretical models proposed [7,13–16] have provided varying insight into the exchange bias phenomenon, but none of them have been able to provide a comprehensive description of all its salient features.

Recently, there has been considerable effort in understanding one of the most important attributes of EB, i.e., the fundamental mechanism of hysteresis, with emphasis on elucidating the intrinsic asymmetry in the magnetization reversal process [8–12]. Even though this asymmetry is now observed in magnetometry measurements of a number of material systems [17,18], much progress in understanding the associated reversal mechanisms has been based on recent studies of a model thin film system TMF_2/Fe (TM is transition metal) [8,9]. Based on interpretations of polarized neutron reflectivity measurements, it is now understood that the magnetic reversal occurs by domain-wall motion on one side of the magnetic hysteresis loop and by magnetization rotation on the opposite side. However, integral to this interpretation of EB in TMF_2/Fe systems is also the presence of a twinned microstructure of the TMF_2 antiferromagnet. In this Letter we demonstrate that this phenomenon is more general by using high quality samples of an alternative model system, MgO/MnPd/Fe, where the underlying antiferromagnet is a single crystal and not twinned in microstructure [19,20]. In addition, we provide real space images of the ferromagnetic domains on either branches of the hysteresis loop, using photoemission electron microscopy (PEEM) [21], as convincing proof of the asymmetry in the reversal mechanism that is beyond the scope of indirect scattering measurements. Direct information of the magnetization distribution of the exchange-biased Fe/MnPd bilayers in the remanent state after saturation along different in-plane crystallographic directions is obtained from the PEEM images.

Thin film heterostructures of MgO/MnPd(380 Å)/Fe(60 Å)/Pt(10 Å) (nominal structure) were grown epitaxially at 375 °C on single-crystalline MgO(001) substrates in an ultrahigh vacuum ion-beam sputter deposition system with a base pressure of 10^{-9} Torr. The composition of the MnPd alloy in the samples was determined by energy dispersive x-ray (EDX) analysis to be Mn(52 at. %)Pd(48 at. %). A magnetic field (300 Oe) was applied along the Fe[100] crystallographic direction during deposition. X-ray diffraction (XRD) texture measurements revealed that the Fe layer is single crystalline with a (001) growth orientation whereas the MnPd layer is single crystalline with a *c*-axis normal orientation, albeit with a very small fraction ($<10\%$) of grains in the *a*-axis normal orientation. A more detailed description of the structural properties of exchange-biased MnPd/Fe bilayers is given in Refs. [19,20].

The microscopy experiments were carried out utilizing the PEEM2 x-ray photoemission electron microscope at the Advanced Light Source. In a photoemission electron microscope the sample is irradiated by x rays of variable polarization and photon energy. The resulting emission of low energy secondary electrons from the surface are then magnified onto a screen by electrostatic lenses and a spatial resolution of typically 50 nm [21] can be achieved. Magnetic contrast of the Fe film is obtained in such a microscope by using circular polarized x rays and acquiring images at the Fe L_3 (706.8 eV) and Fe L_2 (719.9 eV)

core level absorption edges [x-ray magnetic circular dichroism (XMCD)]. Images shown here are the result of a division of these two images. Because the ratio between these two absorption intensities is determined by the projection of the magnetization onto the helicity of the incoming light, it allows for the identification of the direction of the magnetic moments in a domain. The sample was saturated in a magnetic field of 1500 Oe along a specific crystal axis before the magnetic domain images were taken.

Hysteresis loops for the investigated Fe/MnPd sample are shown in Fig. 1. The magnetic field is applied 0° (positive field along Fe[100]) (a), 45° (positive field along Fe[110]) (b), and 90° (c) with respect to the bias direction. The hysteresis loop is shifted when the unidirectional anisotropy has a component along the applied magnetic field while it exhibits an intermediate magnetic state when the unidirectional anisotropy is perpendicular to the field [22,23]. Vibrating-sample magnetometer (VSM) measurements on an exchange-biased MgO/Fe/MnPd/Au sample with pickup coils perpendicular to the applied magnetic field show that this intermediate state corresponds to a net magnetic moment along the bias direction [7]. The hysteresis loops are shifted by -85 Oe (0°) and -75 Oe (45°) while the coercivities are $\sim$200 Oe (0°) and $\sim$110 Oe (45°). The reduced remanence (M_r/M_{tot}) for both the descending and the ascending branch of the hysteresis loop are close to unity when the magnetic field is parallel to the bias direction, 0.89 and 0.85, respectively. No PEEM measurements were therefore carried out for this orientation. When the field is applied at 45° with respect to the bias direction along a magnetic hard direction the reduced remanence is 0.68 (descending) and 0.52 (ascending), respectively. For comparison, in an unbiased Fe(001) film the reduced remanence is the same on both branches and equal to $1/\sqrt{2}$ (0.707...).

PEEM images from the Fe/MnPd bilayer are shown in Fig. 2, where the bottom panel of the figure shows the relationship between the in-plane crystallographic directions, the bias direction (Fe[100]), and the direction of saturation for the three cases studied. It also shows a gray scale legend that links the direction of the magnetization to the image intensity. Note that the gray color corresponds to both horizontal magnetization directions, since XMCD contrast appears between "up" and "down" but not between "left" and "right" domains. The PEEM image for the descending remanent magnetic state after saturation along Fe[110] is shown in Fig. 2(a). No magnetic domains are observed in the image. The very weak features appearing in this otherwise contrastless image are of topographic origin and lead to a variation of the work function which does not completely cancel out in the normalization. The observed domain structure is not related to these features. Thus, the unidirectional anisotropy (or EB) is strong enough to pull the sample magnetization to the bias direction (Fe[100]). In an unbiased Fe(001) film the magnetization along the two magnetic easy directions next to Fe[110] is expected to be equal since the probability for the magnetization to rotate clockwise and counterclockwise is the same.

The corresponding PEEM image for the ascending remanent magnetic state after saturation along the Fe[-1-10] direction is shown in Fig. 2(b). Magnetic domains are in this case clearly visible. The magnetization in the domains is oriented along three of the four in-plane magnetic easy directions: Fe[0-10] (gray), Fe[-100] (black), and Fe[100] (white). As seen, most of the magnetization is along the Fe[0-10] direction, followed by the Fe[-100] and the Fe[100]. The domains with the magnetization along the bias direction (Fe[100]) are due to the induced unidirectional anisotropy; they are not expected in an unbiased Fe(001) film after saturation along Fe[-1-10]. The domains with magnetization parallel and opposite to the bias direction are elongated with a width of $\sim$0.5 μm and a length of $\sim$1–5 μm; moreover, the long axes of these domains are perpendicular to each other with 90° Néel walls oriented along the Fe$\langle 110 \rangle$ directions. This type of domain wall is the most energetically favorable type in ultrathin films with magnetic easy axes oriented 90° with respect to each other. It should be noted that both the elongated shape and the

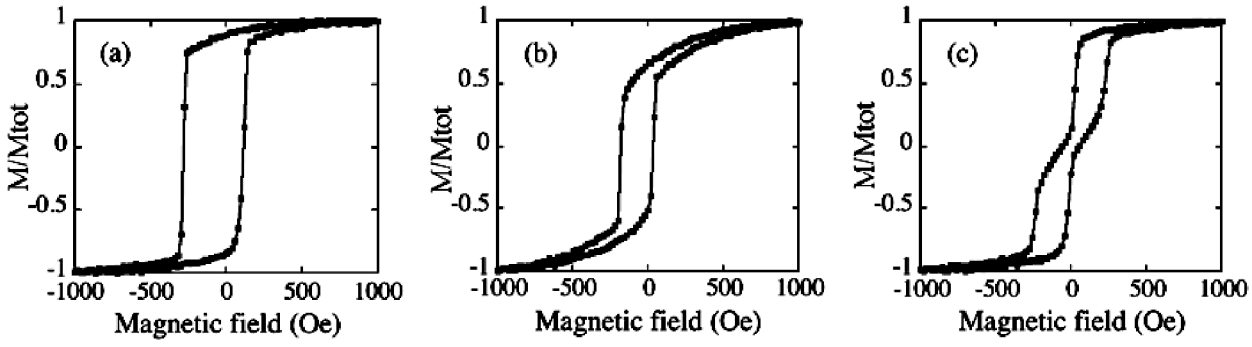

FIG. 1. VSM measurements in the direction parallel to the applied magnetic field. The field is applied 0° (positive field along Fe[100]) (a), 45° (positive field along Fe[110]) (b), and 90° (c) with respect to the bias direction. The hysteresis loop exhibits a shift in (a) and (b), while there is an intermediate magnetic state when the field is perpendicular to the bias direction (c).

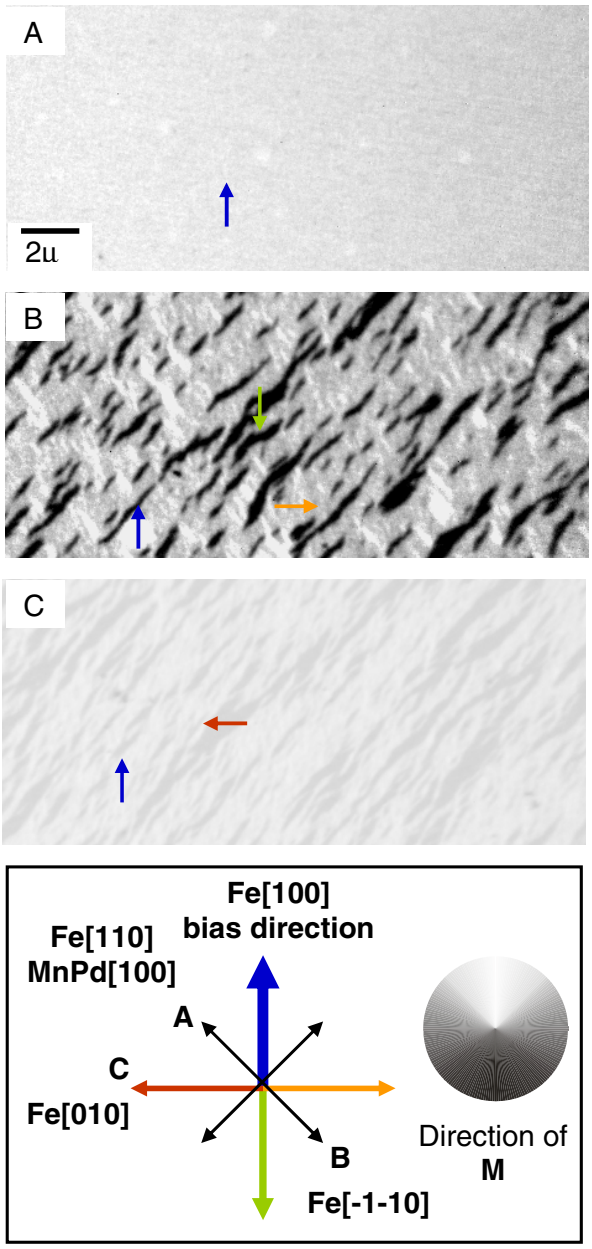

FIG. 2 (color online). PEEM images from the investigated Fe/MnPd bilayer. The sample was saturated in a magnetic field of 1500 Oe along Fe[110] (a), Fe[-1-10] (b), Fe[010] (c), and then measured in zero field. The arrows indicate the direction of the magnetization in the domains. The bottom panel shows the relationship between the in-plane crystallographic directions, the bias direction, and the direction of saturation, while the gray scale legend links the direction of the magnetization (M) to the image intensity.

perpendicular orientation of the Fe[-100] and the Fe[100] domains are due to the fact that most of the sample magnetization is along the Fe[0-10] direction. This means for the Fe[-100] domains that only domain walls parallel to the Fe[1-10] (or equivalently Fe[-110]) direction are energetically favorable. Domain walls parallel to Fe[110] (or Fe[-1-10]) give rise to stray fields because the magnetization is not continuous across these walls. Similarly, for the Fe[100] domains the magnetostatic energy is minimized if the domain walls are oriented along the Fe[110] (or Fe[-1-10]) direction.

PEEM measurements were also carried out after saturation perpendicular to the bias direction along the magnetic easy Fe[010] direction, which means that the intermediate magnetic state in Fig. 1(c) is investigated. Magnetic domains are clearly seen also in this case. The magnetization is either along Fe[100] (white) or Fe[010] (gray), there are in this case no domains with the magnetization opposite to the bias direction. In an unbiased Fe(001) film the magnetization would remain along Fe[010] when the field is reduced to zero because it is a minimum energy state. The Fe[100] domains are due to the unidirectional anisotropy, which is strong enough to pull most of the sample magnetization ($\sim$70%) to the bias direction. The domains are in this case somewhat longer while the width is roughly the same. As in the foregoing measurement, both the elongated shape of the domains and their orientation are a result of minimization of the magnetostatic energy, only domain walls along the Fe[1-10] (or equivalently Fe[-110]) direction are energetically favorable. Interestingly, the same type of stripe domains have also been observed in an epitaxial Fe(001) film after saturation along a magnetic hard Fe$\langle$110$\rangle$ direction [24]. Thus, the PEEM image indicates that the reversal mechanism for this field orientation is domain nucleation and growth and not moment rotation. The symmetric hysteresis loop [Fig. 1(c)] suggests that the reversal mechanism is the same on both branches. For comparison, it has been found that in epitaxial Fe(001) films the magnetization reversal proceeds exclusively by domain nucleation and growth when the magnetic field is applied along one of the magnetic easy axes [25], while in exchange-biased NiO/NiFe bilayers the reversal proceeds by incoherent magnetization rotation when the field is perpendicular to the bias direction [12].

It is evident from the PEEM images that the induced unidirectional anisotropy strongly affects the magnetic domain structure as well as the magnetization processes. As seen in Fig. 2, the images show no magnetic domains after saturation along Fe[110] while a clear domain structure is observed after saturation along the Fe[-1-10] direction. This strongly indicates that the reversal occurs by moment rotation for decreasing magnetic fields and proceeds by domain nucleation and growth for increasing fields. A single-crystalline Fe(001) film exhibits a magnetocrystalline anisotropy with a fourfold symmetry, and the same type of reversal mechanism on both branches of the hysteresis loop. In the exchange-biased Fe/MnPd bilayers, on the other hand, the induced unidirectional anisotropy along the Fe[100] direction breaks this fourfold symmetry. The Fe[100] direction is now the lowest energy state and the Fe[-100] is the highest while the two perpendicular directions (Fe[010] and Fe[0-10]) are intermediate min-

ima. Hence, the observed asymmetry in the magnetization reversal process is therefore most likely a result of the broken symmetry. It should be noted that our results are consistent with recent neutron reflectivity measurements on exchange-biased TMF_2/Fe [8,9] bilayers. However, the opposite behavior has been observed in exchange-biased CoO/Co/Au multilayers; i.e., the main mechanism for decreasing fields is domain-wall motion and moment rotation for increasing fields [10]. The reason for this discrepancy is not completely understood. It has been proposed that the reversal mechanism depends on the properties of the used AFM materials, the strength of the EB, and the thicknesses of the layers [10]. The fact that the strength of the EB and the layer thicknesses of the investigated Fe/MnPd bilayer are much closer to the corresponding values for the TMF_2/Fe bilayers than to the CoO/Co/Au suggests that these parameters are of importance.

In conclusion, we have studied experimentally the remanent magnetic domain structure in high quality, single-crystalline, exchange-biased Fe/MnPd bilayers. Direct imaging by PEEM clearly shows that the exchange bias strongly affects the overall magnetic domain structure. Moreover, we offer direct evidence for an asymmetric magnetization reversal process when the field is applied along the ferromagnetic hard direction. The magnetization reversal occurs by moment rotation for decreasing fields while it proceeds by domain nucleation and growth for increasing fields. The observed domains are consistent with the crystallography of the bilayers and favor a configuration that minimizes the overall magnetostatic energy of the ferromagnetic layer.

The authors would like to thank J. Stöhr and A. Scholl for their support and comments regarding the manuscript. This work was supported by DOE Materials Science Division under Grant No. DE-FG03-02ER45987 and by the Campbell Endowment at UW. Work at the ALS was supported by the Director, Office of Basic Energy Sciences, of the U.S. Department of Energy under Contract No. DE-AC03-76SF00098.

*Corresponding author.
Electronic address: kannanmk@u.washington.edu

[1] W. H. Meiklejohn and C. P. Bean, Phys. Rev. **102**, 1413 (1956).
[2] W. H. Meiklejohn and C. P. Bean, Phys. Rev. **105**, 904 (1957).
[3] For recent reviews, see J. Nogués and Ivan K. Schuller, J. Magn. Magn. Mater. **192**, 203 (1999); A. E. Berkowitz and Kentaro Takano, J. Magn. Magn. Mater. **200**, 552 (1999); Miguel Kiwi, J. Magn. Magn. Mater. **234**, 584 (2001).
[4] C. Leighton, J. Nogues, B. J. Jönsson-Åkerman, and Ivan K. Schuller, Phys. Rev. Lett. **84**, 3466 (2000).
[5] U. Welp, S. G. E. te Velthuis, G. P. Felcher, T. Gredig, and E. D. Dahlberg, J. Appl. Phys. **93**, 7726 (2003); S. G. E. te Velthuis, A. Berger, G. P. Felcher, B. K. Hill, and E. Dan Dahlberg, J. Appl. Phys. **87**, 5046 (2000).
[6] Y. Ijiri, J. A. Borchers, R. W. Erwin, S. H. Lee, P. J. Van der Zaag, and R. M. Wolf, Phys. Rev. Lett. **80**, 608 (1998).
[7] P. Blomqvist, Kannan M. Krishnan, and Er. Girt, J. Appl. Phys. **95**, 8487 (2004).
[8] C. Leighton, M. R. Fitzsimmons, P. Yashar, A. Hoffman, J. Nogues, J. Dura, C. F. Majkrzak, and Ivan K. Schuller, Phys. Rev. Lett. **86**, 4394 (2001).
[9] M. R. Fitzsimmons, P. Yashar, C. Leighton, Ivan K. Schuller, J. Nogues, C. F. Majkrzak, and J. A. Dura, Phys. Rev. Lett. **84**, 3986 (2000).
[10] M. Gierlings, M. J. Prandolini, H. Fritzsche, M. Gruyters, and D. Riegel, Phys. Rev. B **65**, 092407 (2002).
[11] V. I. Nikitenko, V. S. Gornakov, A. J. Shapiro, R. D. Shull, K. Liu, S. M. Zhou, and C. L. Chien, Phys. Rev. Lett. **84**, 765 (2000).
[12] V. I. Nikitenko, V. S. Gornakov, L. M. Dedukh, Yu. P. Kabanov, A. F. Khapikov, A. J. Shapiro, R. D. Shull, A. Chaiken, and R. P. Michel, Phys. Rev. B **57**, R8111 (1998).
[13] A. P. Malozemoff, Phys. Rev. B **37**, 7673 (1988).
[14] N. C. Koon, Phys. Rev. Lett. **78**, 4865 (1997).
[15] T. C. Schulthess and W. H. Butler, Phys. Rev. Lett. **81**, 4516 (1998).
[16] R. L. Stamps, J. Phys. D **33**, R247 (2000).
[17] H. D. Chopra, D. X. Yang, P. J. Chen, H. J. Brown, L. J. Swartzendruber, and W. J. Egelhoff, Phys. Rev. B **61**, 15 312 (2000).
[18] X. Portie, A. K. Petford-Long, A. de Morais, N. W. Owen, H. Laidler, and K. O'Grady, J. Appl. Phys. **87**, 6412 (2000).
[19] Ning Cheng, JaePyoung Ahn, and Kannan M. Krishnan, J. Appl. Phys. **89**, 6597 (2001).
[20] P. Blomqvist, Kannan M. Krishnan, and D. E. McCready, J. Appl. Phys. **95**, 8019 (2004).
[21] A. Scholl, H. Ohldag, F. Nolting, J. Stöhr, and H. A. Padmore, Rev. Sci. Instrum. **73**, 1362 (2002).
[22] Chih-Huang Lai, Yung-Hung Wang, Ching-Ray Chang, Jyh-Shinn Yang, and Y. D. Yao, Phys. Rev. B **64**, 094420 (2001).
[23] Hong-Wu Zhao, W. N. Wang, Y. J. Wang, W. S. Zhan, and J. Q. Xiao, J. Appl. Phys. **91**, 6893 (2002).
[24] U. Ebels, M. Gester, C. Daboo, and J. A. C. Bland, Thin Solid Films **275**, 172 (1996).
[25] E. Gu, J. A. C. Bland, C. Daboo, M. Gester, L. M. Brown, R. Ploessl, and J. N. Chapman, Phys. Rev. B **51**, 3596 (1995).